A case study: The seismic stability of an upstream-raised tailings impoundment (part ii)

Michael James
Department of Civil, Geologic and Mining Engineering, École Polytechnique, Montreal, Quebec, Canada
Nicolas Lemieux, Denise Leahy
SNC-Lavalin Inc., Montreal, Quebec, Canada

ABSTRACT
The seismic stability of an upstream-raised tailings impoundment was evaluated. The impoundment has an exterior shell of compacted, coarse tailings underlain by a drainage system. These elements augment the seismic stability by increasing the liquefaction resistance and limiting seepage pressures in the downstream slope. Analytical liquefaction analysis methods were developed for level ground conditions and may not be applicable given the initial static shear stresses expected within the downstream slope. Furthermore, seismically-induced excess porewater generation in the retained tailings can result in considerable horizontal loads on the retaining dike and the site response may be affected by the geometry of the impoundment. Therefore, numerical rather than analytical methods were used. The evaluation indicates that some zones of high excess porewater pressure development and liquefaction and of minor deformation could be expected within the impoundment but that the risk of instability is extremely low.

RÉSUMÉ
La stabilité sismique d'un parc à résidus miniers été évaluée. Le parc à résidus a une coque extérieure formée de résidus miniers grossiers compactés reposant sur un système de drainage. Ces éléments améliorent la stabilité sismique en augmentant la résistance à la liquéfaction et de limiter les pressions de infiltration dans le talus aval. Les méthodes analytiques d'évaluation du potentiel de liquéfaction ont été développées pour des conditions de terrain horizontal et ne sont peut-être pas applicables ici étant donnée l'importance des contraintes initiales de cisaillement statique prévues dans le talus aval de la digue. De plus, les surpressions interstitielles ou la liquéfaction des résidus dans le parc à résidus générées par un tremblement de terre peuvent imposer à la digue de retenue une charge horizontale importante dont il faut tenir compte. Par conséquent, des méthodes numériques plutôt qu'analytiques ont été utilisées. L'évaluation indique que l'on peut s'attendre au développement de surpressions interstitielles et de déformations limitées dans le parc à résidus et que le risque d'instabilité est extrêmement faible.

1 INTRODUCTION

The paper is Part II of a case study on the seismic stability of an upstream-raised tailings impoundment. Part I (the companion paper) presents the design aspects of the tailings impoundment, construction methods, the results of compaction and in situ testing as well as liquefaction analysis using the Simplified method (Seed and Idriss 1982; Youd et al. 2001).

Mine Niobec is a niobium mine located near Saguenay, Quebec. The tailings produced by the mine are to colloidal to sand size, cohesionless and, when loose and saturated, susceptible to excess porewater generation and liquefaction under seismic loading. Tailings Impoundment No. 2 is currently under construction and is the subject of this paper. The overall plan dimensions of the impoundment are 650 m by 1250 m and the design height is 30 m. Two parallel starter dykes of compacted coarse tailings, spaced 60 m apart, were constructed along the perimeter of the dyke. The area between the dykes is being raised with compacted, coarse tailings in the upstream direction at an inclination of 4:1 (H:V) with the width of the section decreasing to 18 m at a height of 30 m. Fine tailings and total tailings (unsegregated tailings), are being deposited as slurry upstream of the compacted coarse tailings. An internal drainage system was installed at the base of the exterior shell of compacted coarse tailings. The purpose of the exterior shell and the internal drainage system is to improve the static and seismic stability of the impoundment by creating a zone of high shear strength and liquefaction resistance and inhibiting the development of seepage pressures in the downstream slope of the impoundment (Geocon 2003).

The initial compaction method for the coarse tailings consisted of several passes with a loaded 30-tonne-bulldozer on saturated tailings and may have resulted in minor zones of compaction lower than the design criterion, a minimum density index, I_D, of 75%. However, the density index was initially estimated using nuclear density testing that is quite sensitive to the intrinsic variations in the grain size distribution of the tailings and led to some degree of uncertainty in the test results. Subsequently, the compaction method was changed to the cell method and piezocone penetration testing (CPT_u) was used to evaluate the compaction. Additional details on the design, construction, in situ testing, and liquefaction analysis are provided in the companion paper. The focus of this paper is the numerical analysis conducted to evaluate the seismic response and stability of Tailings Impoundment No. 2.

2 METHOD OF ANALYSIS AND EVALUATION

Generally, the numerical modeling of the seismic response of tailings impoundments should be conducted in three phases: 1) a static phase to determine the state of stress and porewater pressure distribution under conditions of mechanical and fluid equilibrium.; 2) a dynamic phase in which the effects of earthquake shaking are simulated; and 3) a post-shaking phase during which the structure returns to a condition of static equilibrium, if possible, by the dissipation of excess porewater pressures, stress redistribution and deformation (Ishihara 1984; James 2009). However, in cases where no significant excess porewater pressures are developed in critical zones (e.g. within the retaining dyke) or where there is no indication of instability at the end of shaking (e.g. ongoing deformation of the downstream slope), the post-shaking phase may not be necessary (James 2009).

Numerical modeling was used to simulate the response of Tailings Impoundment No. 2 to ground motions representative of the expected design earthquake loadings at the site. The response was then evaluated to determine the stability of the impoundment. The elements of response that were evaluated included the horizontal accelerations, cyclic stress ratios, excess porewater pressures, and displacements measured at critical points in the impoundment during shaking as well as the state of stress and deformation of the impoundment at the end of shaking.

The modeling was conducted using version 5 of the FLAC finite difference software program by the Itasca Consulting Group (Itasca 2005).

2.1 Impoundment and Model Geometry

A representative cross-section of the impoundment is presented in the companion paper (Lemieux et al. 2011). It is not presented here due to space limitations. The geometry used in the model was that expected at the completion of the impoundment.

Two foundation conditions were considered. Case 1 consisted of, in descending order, 1 m of clayey topsoil, 4.5 m of normally consolidated clay, and 1.5 m of dense glacial till over limestone bedrock. Case 2 consisted of 1 m of clayey topsoil underlain by 6 m of dense glacial till and then limestone bedrock.

The geometry of the model (Case 1) used in the numerical modeling is shown on Figure 1 and duplicates the planned final geometry quite well.

The model was created on a 20,000 element grid with a typical element size of 1-m-square. The buttresses shown on the ends of the model were placed to provide far field boundaries during the dynamic phases of the analyses.

2.2 Material Models and Properties

Two constitutive models of material behaviour were used in the analysis, the Mohr-Coulomb model and the UBCSAND Model. As implemented in FLAC, the Mohr-Coulomb model is an elasto-plastic model characterized by a c-ϕ failure surface with a tensile yield function and may include post-peak dilatancy (Itasca 2005). The UBCSAND model is a fully coupled elasto-plastic model and was specifically developed to simulate the dynamic response of sand, including excess porewater generation and liquefaction (Byrne et al. 2004).

The Mohr-Coulomb model was used to simulate the response of the limestone bedrock, glacial till, clay, waste rock, and topsoil. The material properties used in the analysis were derived from in situ testing and published sources. The properties are presented in Table 1 and consist of the dry unit weight, γ_{DRY}, the internal friction angle, ϕ', the cohesion, c, the angle of dilation, ψ, the porosity, n, the modulus of elasticity, E, the Poisson's ratio, ν, and the hydraulic conductivity, K. The clay and topsoil were assumed to be normally consolidated under the stresses applied by the impoundment. The cohesion, c, was calculated as 0.25 times the effective vertical stress, σ'_v, and the modulus of elasticity, E, was estimated to be 1000 times the cohesion, c.

Table 1. Properties of Mohr-Coulomb materials.

Property	Limestone	Glacial Till	Clay	Waste Rock	Topsoil
γ_{DRY} (kN/m^3)	23.6	20.7	17.3	21.2	17.3
ϕ' (deg)	40	35	0	38	0
c (kPa)	2.5×10^5	1044	(a)	25	(a)
ψ (deg)	15	0	0	10	0
n	0.11	0.22	0.35	0.20	0.35
E (MPa)	4.3×10^8	5.8×10^5	(a)	3.0×10^6	(a)
ν	0.40	0.40	0.48	0.40	0.48
K (cm/s)	4.6×10^{-4}	5.0×10^{-3}	1.0×10^{-7}	1.0×10^{-3}	1.0×10^{-3}

(a) $c=0.25\cdot\sigma'_v$ and $E=1000\cdot c$

The UBCSAND model was used to simulate the response of the cohesionless materials capable of generating excess porewater pressures during seismic loading. These consisted of all of the tailings and the filter sand. The waste rock was not simulated using the UBCSAND model due to its relatively high hydraulic conductivity and dilatancy.

The key parameters of the UBCSAND model are the corrected standard penetration test (SPT) blow count, $(N_1)_{60}$ and the constant volume friction angle, ϕ_{cv}. The use of the corrected SPT blow count allows the model to be calibrated based on common in situ testing results (SPT or CPT). The constant volume friction angle is related to the resistance of a soil mobilized at the critical state in undrained shear and can be approximated using $(N_1)_{60}$ and the internal friction angle, ϕ' (Byrne et al. 2004).

The properties used for the UBCSAND materials are shown on Table 2. The values of $(N_1)_{60}$ given for the tailings and the lower tailings (the tailings between the

starter dykes) are average values based mainly on piezocone testing described in the companion paper. The values of $(N_1)_{60}$ in these materials were randomized using a standard deviation, σ^2 of 2 blows/30 cm.

The properties given in Table 2 were applied to Cases 1 and 2. A third case, Case 1B, was developed to simulate the effect of relatively lower compaction in the lower tailings (between the starter dykes). In this case, the values of $(N_1)_{60}$ and its standard deviation, σ^2, were 6 and 1 blows/30 cm, respectively. This is a worst case condition and was not based on in situ testing.

Table 2. Properties of UBCSAND materials.

Property	Tailings	Fine Tailings	Coarse Tailings	Lower Tailings	Dykes
γ_{dry} (kN/m^3)	11.0	9.4	19.8	19.8	19.8
$(N_1)_{60}$	6	6	35	14	20
σ^2 $(N_1)_{60}$	2	-	-	2	-
ϕ' (deg)	33	33	36	36	36
n	0.60	0.65	0.25	0.25	0.25
K (cm/s)	3.1×10^{-5}	1.1×10^{-5}	1.4×10^{-4}	1.4×10^{-4}	1.4×10^{-4}

Two types of damping were used in the dynamic phase of the analysis. A hysteric damping function equivalent to that estimated for sand under an effective confining stress of 200 kPa (Seed et al. 1984) was applied to all of the Mohr-Coulomb materials except for Bedrock. The UBCSAND model includes a hysteretic damping function (Byrne et al. 2004). A very minor amount (2%) of Rayleigh stiffness damping was applied to the entire model to provide damping at very low levels of shear strain where hysteretic damping may not be initiated (Cundall 2006).

2.3 Earthquake Loadings

Six earthquake ground motions were used to evaluate the seismic stability of the impoundment. They were based on a recurrence interval of 1,000 years and seismic parameters provided by Earthquakes Canada (2009). Ground motion records from the 1988 Saguenay earthquake were factored to fit specific zones of the expected acceleration response spectrum with Arias intensities similar to that expected from the 1,000-year event. The Arias intensity is a measure of the energy content per unit mass of an earthquake ground motion as it passes through an element of earth and is a more accurate measure of the potential of an earthquake to produce damage than the conventional magnitude/PGA pairing (Kayen and Mitchell 1997).

The results presented here are for the ground motion simulated by factoring record S-16L of the 1988 Saguenay (Quebec) earthquake. The factored ground motion had a peak horizontal acceleration, PGA, of 0.2g, an Arias intensity of 0.25m/s and was equivalent to a magnitude 7 earthquake. This input ground motion is shown on Figure 2. The ground motion measured on the top of bedrock (not shown here) was virtually identical to the input ground motion, indicating that there was no appreciable damping or amplification within bedrock.

The numerical analysis was conducted as follows. The static analysis for Case 1 (normally consolidated clay foundation) was conducted. Next, dynamic analyses of Case 1 using the six earthquake ground motions developed for the site were completed. Case 1B (normally consolidated clay foundation with reduced liquefaction resistance of the lower tailings) was then analyzed for static conditions and the ground motion that resulted in the greatest deformation and excess porewater pressure generation for Case 1. Finally, Case 2 (glacial till foundation) was analyzed for static condition and for the least favourable earthquake loading.

At the end of shaking of the eight dynamic analyses conducted, neither the deformation nor the excess porewater pressure generation was sufficient to require post-shaking analysis to restore mechanical and fluid equilibrium to the model. Had the excess porewater pressures been sufficient to destabilize the downstream slope through seepage pressures induced during dissipation, post-shaking analysis would have been necessary.

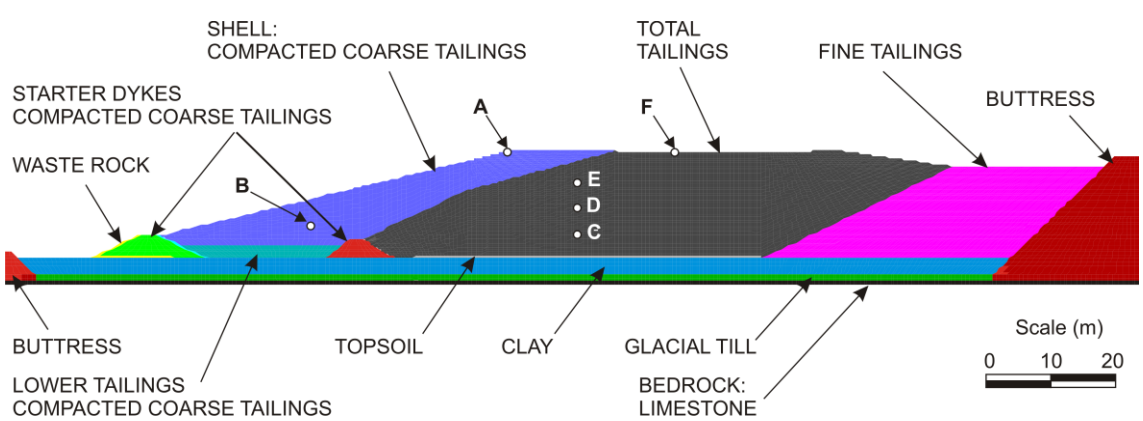

Figure 1. Model of Tailings Impoundment No. 2 used in the numerical analysis (Cases 1 and 1B).

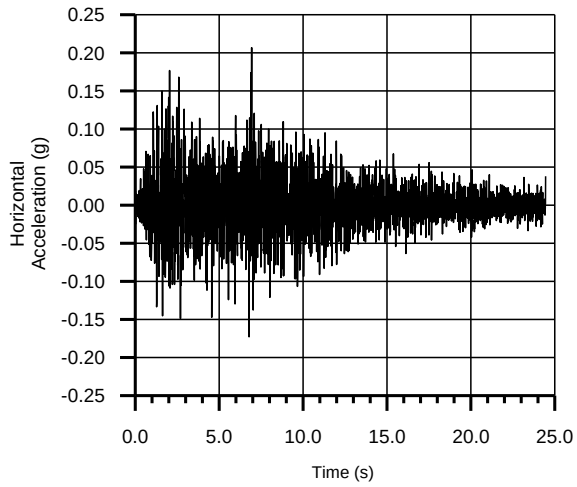

Figure 2. Factored input ground motion based on record S-16L of the 1988 Saguenay earthquake.

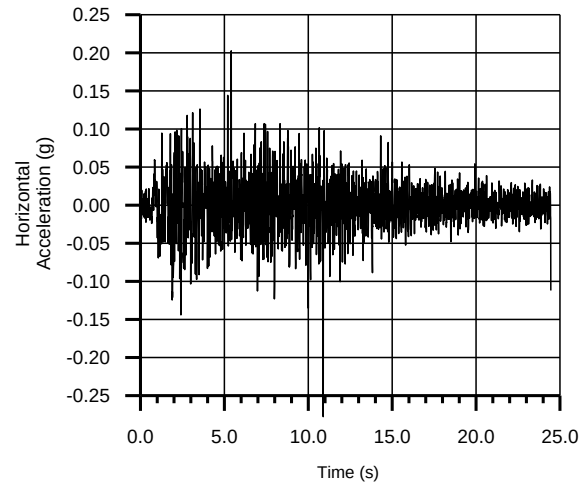

Figure 3. Horizontal accelerations recorded on the crest of the dyke (point A).

3 ANALYSIS AND EVALUATION

Due to space limitations, only selected, representative aspects of the seismic response of the impoundment are presented. Except where stated otherwise, the discussion and figures relate to Case 1B (normally consolidated clay foundation with reduced liquefaction resistance of the lower tailings).

Plots of parameters versus time presented in this paper contain every 25th data point generated during the dynamic analysis (3,640 out of 91,000). As a result, there was a very slight loss of resolution in the plots of horizontal acceleration, cyclic stress ratio, and excess porewater pressure ratio during shaking.

3.1 Horizontal Accelerations

The horizontal accelerations recorded on the crest of the dyke (point A on Figure 1) are shown on Figure 3. By comparing these accelerations with those input to the model (Figure 2), it is evident that there was a moderate amount of alteration of the ground motion as it traveled from bedrock to the top of the compacted shell. Generally, the accelerations were dampened during shaking. However, there were some isolated points of amplification during the 5th, 10th and 24th seconds of shaking. The isolated peak amplifications on the crest of the dyke are not significant because their very small wave length indicates an insignificant amount of energy.

Generally, ground motions are amplified on the crest of earth dams due to the geometry and damped on the surfaces of tailings impoundments due to shear strain in the relatively soft tailings (Cascone and Rampello 2003; James 2009). In this case, the ground motion was dampened on the crest of the dike. The damping is attributed to the relatively softer tailings underlying the compacted tailings shell in the area of the crest.

The horizontal accelerations recorded on the top of the clay layer (bottom of the tailings) are plotted on Figure 4. Based on a comparison with Figure 2, there was a minor amount of amplification of the ground motion as it traveled from the bedrock to the top of the clay.

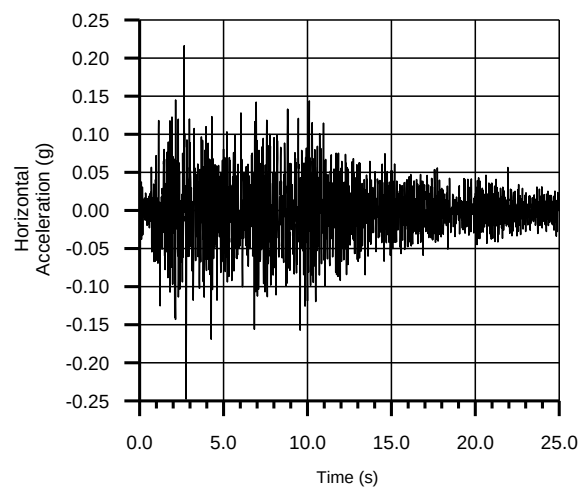

Figure 4. Horizontal accelerations recorded on the top of the clay layer.

Amplification is the expected response as a ground motion travels from a layer to less stiff layer, provided the less stiff layer does not undergo significant shear strains or excess porewater pressure generation that would induce damping.

Figure 5 presents the horizontal accelerations recorded on the surface of the impoundment (point F in Figure 1). It is evident that the ground motion was significantly damped as it passed through the tailings. The damping may be indicative of shear strain and excess porewater pressure generation in the tailings. These aspects are described below.

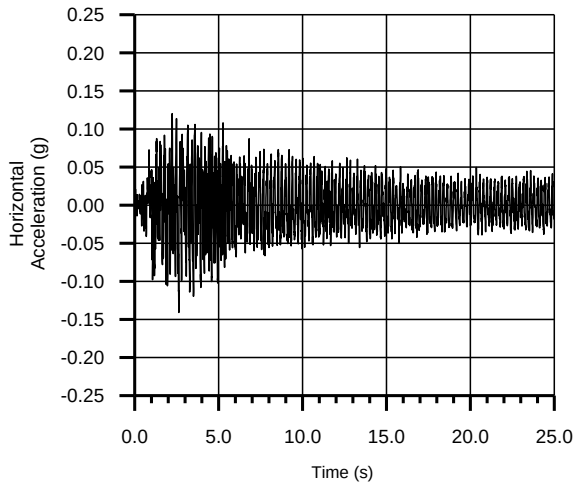

Figure 5. Horizontal accelerations recorded on the top of the impoundment (point F).

3.2 Cyclic Stress Ratio Development

As noted in the companion paper, the seismic loading of an earthquake on an element of soil can be defined using the cyclic stress ratio, CSR, which is the ratio of the shear stress directly applied by the earthquake loading, τ, to the initial effective vertical stress, $\sigma'_{v,0}$. In the simplified method of liquefaction analysis (Seed and Idriss 1982), the applied shear stress is solely the loading applied by the earthquake. In the numerical analysis, the shear stress used to calculate the CSR includes the shear stress directly due to the earthquake loading as well as the initial static shear stress and any shear stress applied due to the response of the impoundment.

The cyclic stress ratio calculated during shaking at point B, about mid-height in the compacted coarse tailings, is presented on Figure 6. At point B there was an initial static shear loading equal to about 0.125 times the initial effective vertical stress. During shaking, the amplitudes of the CSR variation were as great as 0.1 but generally between 0.025 and 0.075. There was also a general increase in the CSR from 0.125 at the start of shaking to 0.2 at the end of shaking. This increase is attributed to shear loading of the impoundment on the shell of compacted tailings in response to the earthquake loading.

The CSR values calculated at point C, D and E in the retained tailings are presented on Figure 7. The initial static shear stresses at these locations were relatively low, 0.03 to 0.04, indicating approximate level ground conditions.

In the lower part of the tailings (point C), the amplitudes of CSR variation were generally less than 0.1 for the first 3 seconds of shaking and about 0.01 for the remaining duration of shaking. At mid-height (point D) the amplitudes of CSR variation were 0.05 or less for the duration of shaking. At point E (the upper part of the tailings), the amplitudes of CSR variation were generally about 0.1 for the first ten seconds of shaking and about 0.05 for the rest of shaking. It's interesting to note that a CSR of 0.05 is considered to be the lower limit at which significant excess porewater pressures can be developed (Carter and Seed 1988).

The CSR values developed at point E may have been influenced by the proximity of the relatively stiffer compacted tailings shell. The general trend of the CSR values shows that there was no other significant shear loading on the tailings due to earthquake shaking.

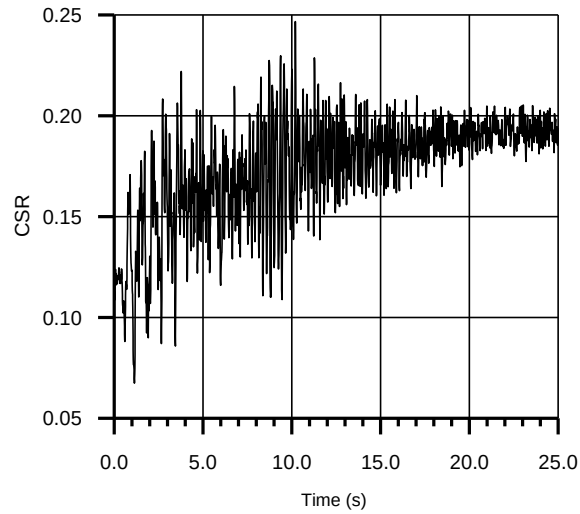

Figure 6. Calculated CSR values at point A in the compacted tailings during shaking.

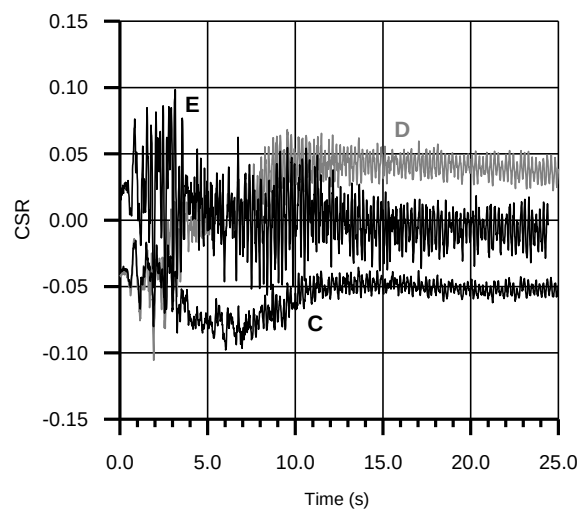

Figure 7. Calculated CSR values at points C, D and E in the retained tailings during shaking.

3.3 Excess Porewater Pressure Development and Liquefaction

The excess porewater pressure development was monitored through the use of the excess porewater pressure ratio, r_u. This is usually defined as the ratio of the change in porewater pressure to the initial vertical effective stress, $\Delta u/\sigma'_{v,0}$. However, in this analysis r_u was defined as the ratio of the change in the vertical effective stress to the initial vertical effective stress, $\Delta\sigma'_v/\sigma'_{v,0}$. This

definition allows monitoring of changes to the vertical effective stress from all sources and can result in negative values and values greater than 1.0 due to stress redistribution during shaking.

The r_u values measured at point B (compacted coarse tailings) during shaking are plotted on Figure 8. The r_u values varied with the cyclic stress ratio and with an overall increase to 0.08 during shaking. This minor increase relative to the CSR induced (Figure 4) is attributed to the liquefaction resistance provided by compaction, $(N_1)_{60}$=35 blows/30 cm.

The r_u values measured at points C, D and E (retained tailings, $(N_1)_{60}$=6 blows/30 cm) during shaking are shown on Figure 9. In the lower part of the tailings (point C) there was no significant change in the value of r_u during shaking. At points D and E, the excess porewater pressure ratio increased to 0.3 by the 10th second of shaking and remained constant for the duration. The moderate increase in r_u values at D and E are in agreement with the CSR values developed (Figure 7). However, the increase at D appears to be related to shear loading of the tailings not directly attributed to the cyclic loading of the earthquake. The amplitudes of the CSR at D were not as great as those at E, but there was an appreciable increase in the shear loading between the 2nd and 8th seconds of shaking.

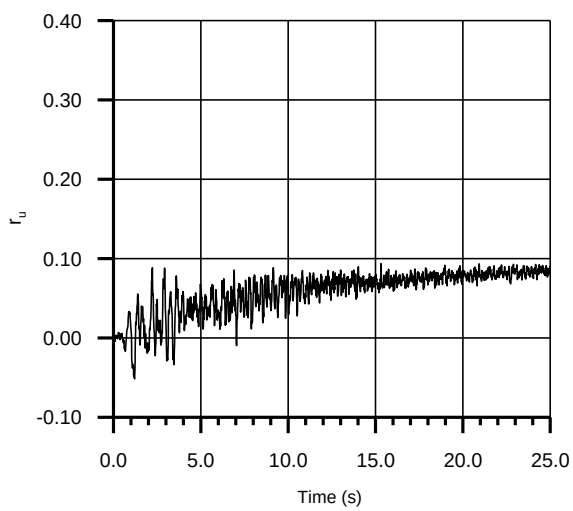

Figure 8. Calculated r_u values at point B in the compacted coarse tailings during shaking.

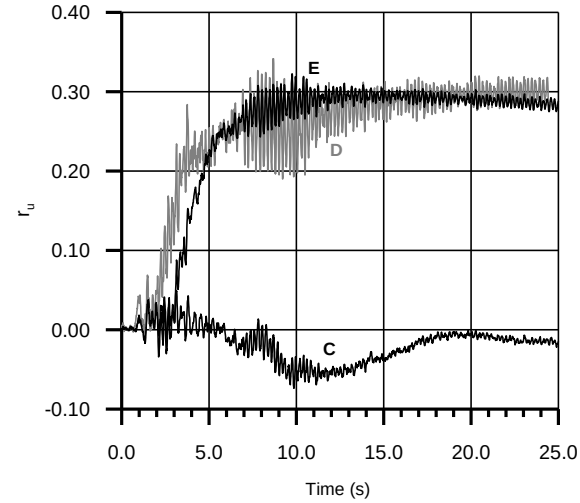

Figure 9. Calculated r_u values at points C, D and E in the retained tailings during shaking.

The development of excess porewater pressures in the impoundment during shaking is shown on Figures 10 and 11 that respectively show the porewater pressure distributions in the impoundment before and after earthquake shaking. The greatest increase in porewater pressure occurred in the bottom of the retained tailings where porewater pressure increased by about 140 kPa during shaking. There was no significant increase in the porewater pressures in the area of downstream slope, except in the lower tailings (between the starter dykes) where porewater pressures increased by about 50 kPa.

Figure 12 presents the excess porewater pressure ratio distribution in the impoundment at the end of shaking. Values of r_u approaching 1.0 were developed in the upper 5 to 10 m of the total tailings and for most of the depth of the fine tailings. In the lower tailings, r_u values may have been as great as 0.5.

If liquefaction is defined as an r_u value of 1.0, based on Figure 12, limited zones liquefaction occurred in the retained tailings during shaking, particularly in the fine tailings. There were no zones of liquefied material (or high excess porewater pressure development) in the vicinity of the downstream slope.

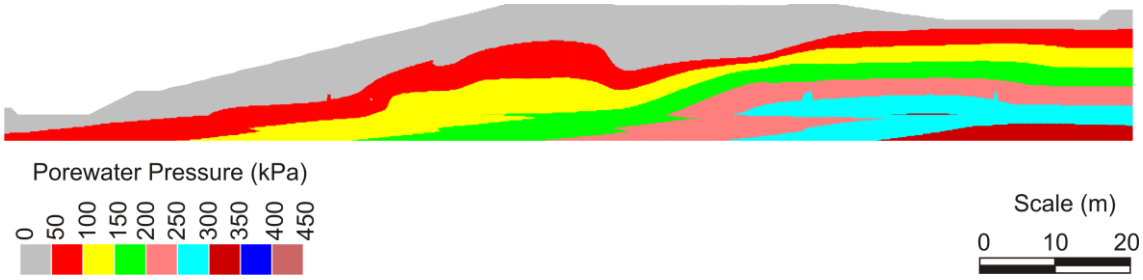

Figure 10. Porewater pressure distribution in the model under static conditions (before earthquake shaking).

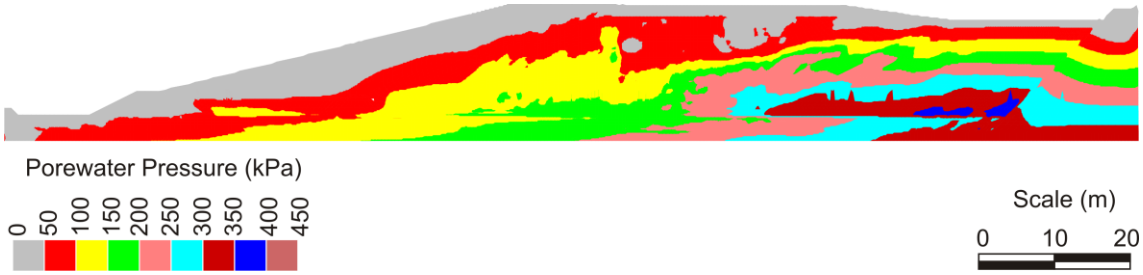

Figure 11. Porewater pressure distribution in the model at the end of shaking.

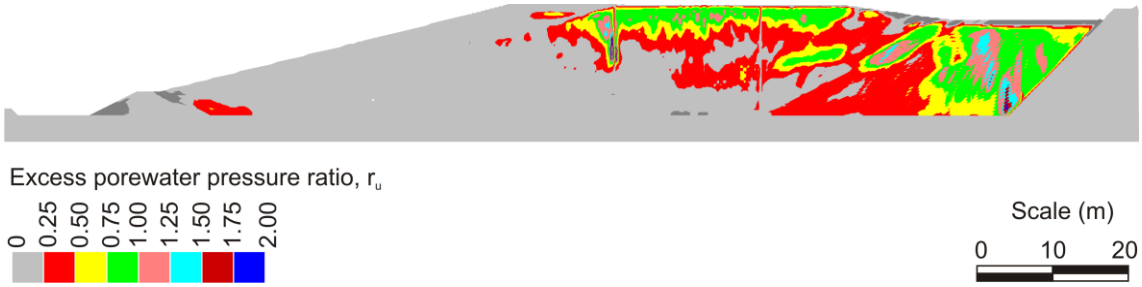

Figure 12. Excess porewater pressure ratio, r_u at the end of shaking.

3.4 Deformation and Displacements

The horizontal displacements in the impoundment at the end of shaking are presented on Figure 13. Deformation of the impoundment during shaking was generally limited to the slope at the boundary between the tailings and the fine tailings, 50 m upstream of the crest, where a maximum deformation of approximately 0.7 m occurred. There was no significant deformation of the downstream slope of the impoundment. There were no significant vertical displacements of the impoundment.

The displacement of the crest of the impoundment (point A) at the end of shaking was 5 cm in the downstream direction and 0.3 cm downwards. The relatively minor displacements of the crest are attributed to the rigidity of the compacted coarse tailings shell.

3.5 Seismic Stability Evaluation

The seismic stability of the impoundment was evaluated based on: a) The pattern of deformation and magnitude of displacements of the impoundment during shaking, particularly of the downstream slope and crest; b) The magnitude and extent of excess porewater pressure generation and liquefaction in the vicinity of the downstream slope; and c) The velocities of the elements of the model at the end of shaking.

As noted above, deformation and displacement of the downstream slope and crest were negligible, there was no significant excess porewater pressure generation in the shell of compacted, coarse tailings and excess porewater pressure generation in the retained tailings was generally moderate. Based on this, there was no need to conduct post-shaking analysis.

At the end of shaking, the velocities on the downstream slope of the impoundment were less than 0.006 m/s in the downstream direction. This level of velocity is not indicative of failure. It represents residual movement of the structure following shaking.

Given the response of the impoundment to the simulated earthquake ground motion, the risk of failure during an equivalent seismic event is extremely low.

Figure 13. Horizontal displacement of the impoundment at the end of shaking.

3.6 Cases 1 and 2

The responses of the tailings impoundment for Cases 1 and 2 were quite similar to that of Case 1B that is described above. In Case 1 and 2 there was less excess porewater pressure development in the tailings between the starter dykes and in Case 2 (glacial till overburden) there was more amplification of the ground motion between the top of bedrock and the bottom of the tailings and more deformation of the retained tailings. The horizontal deformation of the retained tailings for Case 2 was as much as 1.5 m. The horizontal displacements of the crest for Case 2 were 7.2 cm downstream and 0.2 cm downwards.

4 DISCUSSION AND CONCLUSIONS

The seismic response of a tailings impoundment depends on many inter-related factors that cannot be modeled using existing analytical methods. For example, the transmission of the horizontal accelerations is influenced by the initial material properties, impoundment geometry, state of stress, shear strain (resulting in damping and shear modulus reduction), and the development of excess porewater pressures. Yet these phenomena, except for the initial material properties and geometry, are either produced or significantly altered by the horizontal accelerations and the shear stresses they produce. Numerical modeling is capable of simulating this interaction and providing a reasonable estimate of the response of an earth structure to seismic loading. However, due to the random characteristics of seismic activity and the limitations inherent in even the most advanced numerical modeling, the results of numerical modeling may be used to evaluate the overall performance or parametric analysis, but are not suitable as a predictive tool.

For Tailings Impoundment No. 2 at Mine Niobec, numerical analysis using six different ground motions and three representative cases indicated acceptable performance of the structure for the design earthquake.

ACKNOWLEDGEMENTS

The authors acknowledge and appreciate the permission granted by IAMGOD, Division Niobec, for the publication of this case study and their assistance during the project.

REFERENCES

Byrne, P.M., Park, S.S. and Beaty, M., Sharp, M., Gonzalez, L., and Abdoun, T. 2004. Numerical Modeling of Liquefaction and Comparison with Centrifuge Tests. *Canadian Geotechnical Journal*, 41, 191-211.

Carter, D.P. and Seed, H.B. 1988. *Liquefaction of Sand Deposits Under Low Levels of Excitation (Report No. EERC 88/11).* Earthquake Engineering Research Center, Berkeley, CA.

Cascone, E. & Rampello, S. (2003). Decoupled Seismic Analysis of an Earth Dam. Soil Dynamics and Earthquake Engineering. 23(5). pp. 349-365.

Cundall, P.A. 2006. A Simple Hysteretic Damping Function Formulation for Dynamic Continuum Simulations. *FLAC and Numerical Modeling in Geomechanics*, Itasca Consulting Group, Madrid, Spain, 359-364.

Earthquakes Canada. 2009. Seismic Hazard Calculations and Deaggregation Reports (www.earthquakescanada.ca).

Geocon. 2003. Conception du parc a résidus no. 2, Service Minéraux Industriels Inc., La Mine Niobec, Report M-6677 (602906-7000).

Ishihara, K. (1984). Post-Earthquake Failure of a Tailings Dam due to Liquefaction of the Pond Deposit. Proceedings of the International Conference on Case Histories in Geotechnical Engineering, St-Louis USA, (pp. 1129-1143). New York: ASCE.

Itasca Consulting Group Inc. (Itasca). 2005. FLAC – Fast Lagrangian Analysis of Continua. Version 5.00.377 [computer software and user manual]. Minneapolis, MN.

James, M. 2009. The Use of Waste Rock Inclusions to Control the Effects of Liquefaction in Tailings Impoundments. Unpublished Ph.D. Thesis, Ecole Polytechnique, Montreal, Quebec.

Kayen, R.E. and Mitchell, J.K. 1997. Assessment of Liquefaction Potential During Earthquakes by Arias Intensity. *Journal of Geotechnical and Geoenvironmental Engineering*, ASCE, 133: 1162-1174.

Seed, H.B. and Idriss, I.M. 1982. Ground Motions and Soil Liquefaction During Earthquakes. Berkeley CA: Earthquake Engineering Research Institute.

Seed, H. B., Wong, R. T., Idriss, I. M. & Tokimatsu, K. (1984). Dynamic Moduli and Damping Factors for Dynamic Analysis of Cohesionless Soils (Report No. UCB/EERC-84/14). Berkeley CA: Earthquake Engineering Research Center.

Youd, T. L., Idriss, I. M., Andrus, R. D., Arango, I., Castro, G., Christian, J. T. et al. (2001). Liquefaction Resistance of Soils: Summary Report from the 1996 NCEER and 1998 NCEER/NSF Workshops on Evaluation of Liquefaction Resistance of Soils. Journal of Geotechnical and Geoenvironmental Engineering, 127(10), 817-833.